THE AMERICAN MINERALOGIST, VOL. 55, NOVEMBER–DECEMBER, 1970

GEDRITES: CRYSTAL STRUCTURES AND INTRACRYSTALLINE CATION DISTRIBUTIONS

J. J. PAPIKE, *Department of Earth and Space Sciences, State University of New York, Stony Brook, New York 11790*
AND
MALCOLM ROSS[1], *U. S. Geological Survey, Washington, D. C. 20242*

ABSTRACT

The crystal structures of two aluminous and sodic orthoamphiboles (gedrites) have been refined. Most of the sodium occupies the A-site, where it is tightly coordinated by six oxygen atoms, and shows little positional disorder. This contrasts with sodium in the A-site of clinoamphiboles, where sodium shows a high degree of positional disorder and irregular coordination. The significant difference in A-site coordination between clino- and orthoamphiboles results from difference in stacking of the tetrahedral chains around the site. A chain direction can be defined in terms of the trigonal aspect of the six-membered rings of tetrahedra. In clinoamphiboles the chains point in opposite directions above and below the site ($+c$, $-c$) whereas in these orthoamphiboles both chains are identically directed ($+c$, $+c$, or $-c$, $-c$). Tetrahedral aluminum is disordered over three of the four distinct tetrahedral sites in these gedrites. The fourth is mainly occupied by silicon. The tetrahedron occupied by silicon shares an edge with an $M(4)$ octahedron and is inherently small in size. Octahedral aluminum is concentrated in the $M(2)$ site in these structures, while ferrous iron prefers the $M(4)$ site over the $M(1)$, $M(2)$, and $M(3)$ sites. Differences in the iron-magnesium distributions in the gedrites from two different localities suggest a difference in thermal history.

INTRODUCTION

In many respects gedrites are the most crystal-chemically complex amphiboles and this may be why their detailed characterization has been accomplished only recently. A general formula for gedrite, $Na_xR_2^{2+}(R_{5-y}^{2+}R_y^{3+})(Si_{8-x-y}Al_{x+y})O_{22}(OH,F)_2$, where $R^{2+}=Fe^{2+}+Mg+Mn$ and $R^{3+}=Al+Fe^{3+}$, was proposed by Robinson, Ross, and Jaffe (1970). Two important coupled substitution mechanisms are represented in this formula: first is the substitution of Na into the normally vacant A-sites coupled with replacement of Al for Si in the T-sites; second is a substitution of R^{3+} for R^{2+} in the M-sites coupled with substitution of Al for Si in the T-sites. The data of Robinson *et al.* (1970) clearly show the importance of both substitutions.

The first crystal structure of an orthoamphibole to be solved was that of anthophyllite by Warren and Modell (1930). Since that time a two-dimensional solution of the holmquistite structure has been presented by Whittaker (1969) and a three-dimensional refinement of an anthophyllite has been presented by Finger (1970a,b). Cation distributions in an

[1] Publication authorized by the Director, U.S Geological Survey.

anthophyllite have been studied by Bancroft and Strens (1966) using spectral techniques.

Gedrite (Sample No. 001) selected for this study is from high-grade metamorphic rocks of Mason Mountain, North Carolina, described by Henderson (1931), Heinrich (1950), and Barker (1961). This locality was also referred to by Rabbitt (1948) in his comprehensive study of the anthophyllite series. According to Heinrich (1950) and Barker (1961) the primary minerals in this deposit were rhodolite (a pyrope-rich variety of garnet) and hypersthene. Barker suggests that these minerals went through a middle-rank metamorphic event and that gedrite, biotite, quartz, and sillimanite formed during a second, high-rank metamorphism. Gedrite (Sample No. 002, Robinson and Jaffe No. 134I) is from high-grade sillimanite-bearing metamorphic rocks from the Richmond, New Hampshire, locality described by Robinson and Jaffe (1969a, 1969b). The mineral assemblage cited by these authors includes quartz, gedrite, sillimanite, kyanite, staurolite, biotite, garnet, and ilmenite. Robinson (1966) has estimated conditions of metamorphism at 650°C and 6 b.

Experimental Data

Unit-cell parameters, space groups, chemical analyses, and calculated unit-cell contents are presented in Table 1. Although Henderson (1931) reported a wet chemical analysis for the Mason Mountain gedrite he did not analyze for Na. His analyses did show, however, that Fe^{3+} is fairly low, and therefore our calculation of the gedrite formula based on electron microprobe data is a fair approximation. Collection and correction of the X-ray diffraction data are done according to methods described by Clark, Appleman, and Papike (1969). Table 2 presents information on size of crystals, details of the experimental procedure, number of $|F_o| > 0$, and final $R = \Sigma[|F_o| - |F_c|]/\Sigma|F_o|$.

The refinements for both gedrites were initiated with positional parameters for anthyphyllite (Finger, 1970b). The computer programs used for the refinements were those of Dr. L. W. Finger, Geophysical Laboratory, Washington, D. C. The bond distances, angles, and errors were calculated with J. M. Stewart's (University of Maryland) X-ray 67, Program System for X-ray Crystallography (1967) adapted by D. E. Appleman, U. S. Geological Survey, for the IBM 360/65 computer. Atomic scattering factors used during the refinement were those of Cromer and Waber (1965) and the method of site-occupancy refinement is that described by Finger (1969b).

Although there are good reasons for predicting space groups other than *Pnma* for orthoamphiboles (Thompson, 1970) we observed no violations of *Pnma* symmetry either in long exposure precession photographs or with the diffractometer. The only space group that has the same

TABLE 1. CRYSTAL DATA FOR TWO GEDRITES

	Gedrite 001	Gedrite 002
a(Å)	18.531±0.004	18.601±0.004
b(Å)	17.741±0.004	17.839±0.003
c(Å)	5.249±0.005	5.284±0.002
Cell volume (Å^3)	1725.8±1.4	1753.2±0.6
Space group	*Pnma*	*Pnma*
	Unit cell contents	
Si	6.25	5.953 (includes 0.005P)
Al^{IV}	1.75	2.047
Tetrahedral Σ	8.00	8.000
Al^{VI}	1.21	1.365
Mg	4.52	3.009
Fe^{2+}	1.14	2.351
Fe^{3+}		0.140
Mn	0.02	0.031
Ti	0.06	0.026
Li	—	0.018
Cr	—	0.002
Octahedral Σ	6.95	6.942
Ca	0.03	0.042
Na	0.47	0.544
K	—	0.007
Large cation Σ	0.50	0.593
Z	4	4
Calc. density g/cm^3	3.18	3.29
Locality	Mason Mountain, North Carolina	Southern New Hampshire
Information on analyses	Analyst A. T. Anderson (electron microprobe) Na_2O 1.78, FeO 9.93, MgO 22.09, CaO 0.22, SiO_2 45.52, Al_2O_3 18.33, MnO 0.13, TiO_2 0.62, Σ 98.62	Robinson and Jaffe (1969)
Unit cell content Calculation based on:	22 oxygens +2(OH)	22 oxygens +2(OH)

TABLE 2. DATA COLLECTION INFORMATION FOR TWO ORTHOAMPHIBOLES

	Gedrite 001	Gedrite 002
Size of crystal volume in cm^3	0.1039×10^{-5}	0.2420×10^{-5}
Radiation/filter	Mo/Nb	Mo/Nb
Collection method	[a]	[a]
Crystal axis for data collection	C^*	C^*
Absorption correction	Yes	Yes
μcm^{-1}	19.5	29.5
No. of $\|Fo\| > 0$	1417	1503
Weighting scheme used	unit weights	unit weights
Definition of $\|Fo\|$	4×S.D. of background	4×S.D. of background
Final R	0.076	0.072

[a] Normal-beam equatorial 4-circle automatic diffractometer, scintillation counter, 2θ scan.

extinction criteria is $Pn2_1a$. However, refinement attempts in this space group did not improve the model and therefore the structures of the two gedrites consistent with *Pnma* symmetry are presented.

The results of the two gedrite refinements are reported as follows: Table 3, final positional parameters and isotropic temperature factors; Table 4[1] observed and calculated structure factors; Table 5, interatomic distances for tetrahedral chains; Table 6, interatomic angles in tetrahedral chains; Table 7, interatomic distances between oxygen atoms and the A- and M-site occupants; Table 8, selected interatomic angles for the M- and A-sites.

TOPOLOGICAL ASPECTS OF GEDRITE STRUCTURES

Before considering the problem of cation distributions over the crystallographically distinct sites in gedrite (Topochemistry) we will compare the topology of the orthoamphibole structures to that of other amphibole structures. Specifically, we will emphasize the various amphibole structure model possibilities resulting from tetrahderal chain rotations and octahedral chain stacking sequences.

Thompson (1970) pointed out two distinct possibilities for the relationship between a tetrahedral double chain and the adjacent octahedral strip. These two possibilities, referred to as S-rotations and O-rotations, are illustrated for amphiboles in Figures 1 and 2. In S-rotations the tetrahedra in the chains rotate so that the triangular faces (those approx-

[1] Table 4 may be ordered as NAPS Document No. 01255 from National Auxiliary Publications Service of ASIS, c/o CCM Information Corporation, 909 Third Avenue, New York, New York 10022, remitting $2.00 for microfiche or $5.00 for photocopies, payable to CCMIC-NAPS.

TABLE 3. FINAL POSITIONAL PARAMETERS AND TEMPERATURE FACTORS FOR TWO ORTHOAMPHIBOLES

Atom	Parameter	Gedrite 001		Gedrite 002	
		A-Set	*B*-Set	*A*-Set	*B*-Set
O(1)	*x*	0.1796 (4)	0.0695 (5)	0.1790 (4)	0.0701 (4)
	y	0.1603 (4)	0.1584 (5)	0.1581 (4)	0.1568 (4)
	z	0.0312 (15)	−0.2860 (17)	0.0315 (15)	−0.2900 (15)
	B(Å²)	0.40 (10)	0.92 (12)	0.78 (11)	0.76 (10)
O(2)	*x*	0.1840 (5)	0.0622 (4)	0.1850 (4)	0.0635 (4)
	y	0.0737 (5)	0.0742 (4)	0.0731 (4)	0.0739 (4)
	z	−0.4436 (18)	0.1875 (14)	−0.4409 (15)	0.1808 (15)
	B(Å²)	1.05 (12)	0.50 (10)	0.80 (11)	0.85 (11)
O(3)	*x*	0.1797 (7)	0.0700 (6)	0.1811 (6)	0.0701 (6)
	y	0.25	0.25	0.25	0.25
	z	−0.4571 (27)	0.2087 (23)	−0.4662 (22)	0.2111 (22)
	B(Å²)	1.02 (19)	0.75 (16)	0.77 (16)	0.90 (16)
O(4)	*x*	0.1868 (4)	0.0679 (4)	0.1863 (4)	0.0685 (4)
	y	0.0022 (4)	−0.0046 (4)	0.0028 (4)	−0.0049 (4)
	z	0.0425 (16)	−0.2985 (16)	0.0445 (16)	−0.2986 (15)
	B(Å²)	0.62 (11)	0.74 (11)	0.85 (11)	0.86 (11)
O(5)	*x*	0.1968 (5)	0.0549 (4)	0.1973 (4)	0.0545 (4)
	y	−0.1090 (5)	−0.1026 (4)	−0.1100 (4)	−0.1014 (4)
	z	0.3206 (17)	0.0943 (15)	0.3215 (14)	0.0989 (14)
	B(Å²)	1.06 (12)	0.72 (11)	0.78 (10)	1.01 (11)
O(6)	*x*	0.2022 (4)	0.0472 (5)	0.2030 (4)	0.0473 (4)
	y	−0.1313 (4)	−0.1450 (5)	−0.1320 (4)	−0.1461 (4)
	z	−0.1752 (15)	−0.4097 (18)	−0.1763 (16)	−0.4036 (15)
	B(Å²)	0.73 (11)	1.49 (15)	1.12 (11)	1.10 (12)
O(7)	*x*	0.2030 (6)	0.0454 (7)	0.2050 (6)	0.0453 (6)
	y	−0.25	−0.25	−0.25	−0.25
	z	0.5138 (21)	0.2153 (26)	0.5141 (22)	0.2154 (21)
	B(Å²)	0.65 (16)	1.31 (19)	1.18 (18)	0.77 (15)
T(1)	*x*	0.2315 (2)	0.0202 (2)	0.2323 (1)	0.0199 (1)
	y	−0.1631 (2)	−0.1645 (2)	−0.1626 (2)	−0.1641 (2)
	z	−0.4487 (6)	0.2971 (6)	−0.4505 (6)	0.3018 (5)
	B(Å²)	0.43 (4)	0.42 (4)	0.56 (4)	0.50 (4)
T(2)	*x*	0.2278 (2)	0.0266 (2)	0.2282 (1)	0.0268 (1)
	y	−0.0760 (2)	−0.0802 (2)	−0.0759 (2)	−0.0799 (2)
	z	0.0502 (6)	−0.1985 (6)	0.0509 (6)	−0.1947 (6)
	B(Å²)	0.46 (4)	0.58 (4)	0.44 (4)	0.59 (4)

TABLE 3.—(*Continued*)

Atom	Parameter	Gedrite 001		Gedrite 002	
		A-set	*B*-set	*A*-set	*B*-set
M(1)	*x*	0.1244 (2)		0.1242 (1)	
	y	0.1611 (2)		0.1603 (1)	
	z	0.3737 (8)		0.3705 (5)	
	B(Å²)	0.75 (7)		0.71 (5)	
M(2)	*x*	0.1248 (2)		0.1247 (1)	
	y	0.0731 (2)		0.0724 (2)	
	z	−0.1281 (7)		−0.1290 (6)	
	B(Å²)	0.34 (7)		0.30 (6)	
M(3)	*x*	0.1249 (3)		0.1243 (2)	
	y	0.25		0.25	
	z	−0.1248 (10)		−0.1294 (7)	
	B(Å²)	0.47 (10)		0.57 (7)	
M(4)	*x*	0.1189 (1)		0.1184 (1)	
	y	−0.0145 (1)		−0.0153 (1)	
	z	0.3636 (5)		0.3635 (4)	
	B(Å²)	0.63 (4)		0.62 (3)	
A	*x*	0.1151 (13)		0.1171 (8)	
	y	−0.25		−0.25	
	z	0.8533 (47)		0.8480 (27)	
	B(Å²)	1.47 (49)		1.53 (30)	

imately normal to a^*) of the tetrahedra are similarly directed to the triangular faces of the octahedral strip to which they are linked. In *O*-rotations the tetrahedra rotate so that the triangular faces of the tetrahedra are directed opposite to the triangular faces of the octahedra. Similar types of rotations have been recognized in micas by Franzini and Schiaffino (1963) and Franzini (1969). Figure 1A illustrates that a completed *S*-rotation results in hexagonal close packing of oxygens (*ABAB*) and Figure 1B illustrates that completed *O*-rotations result in cubic close packing of oxygens (*ABCABC*).

Tetrahedral chains in which there are no *O*- or *S*-rotations will have O(5)–O(6)–O(5) bond angles of 180° (Fig. 4)[1] and the hexads of SiO_4 tetrahedra will possess 6-fold symmetry. Tetrahedral chains which show

[1] For the purposes of this papter the relative amount of rotation of the tetrahedra will be defined in terms of the magnitude of the O(5)–O(6)–O(5) bond angle (Figs. 1 and 4).

TABLE 5. INTERATOMIC DISTANCES IN TETRAHEDRAL CHAINS FOR TWO ORTHOAMPHIBOLES

T–O distances (Å)

Atoms	Gedrite 001		Gedrite 002	
	A-Chain	*B*-Chain	*A*-Chain	*B*-Chain
T(1)–O(1)	1.651 (8)	1.665 (9)	1.653 (8)	1.679 (8)
T(1)–O(5)	1.673 (9)	1.658 (8)	1.660 (8)	1.677 (8)
T(1)–O(6)	1.635 (9)	1.654 (10)	1.641 (9)	1.668 (8)
T(1)–O(7)	1.640 (5)	1.643 (6)	1.649 (5)	1.666 (5)
Average	1.650	1.655	1.651	1.672
T(2)–O(2)	1.635 (9)	1.648 (8)	1.613 (7)	1.683 (8)
T(2)–O(4)	1.579 (8)	1.630 (8)	1.605 (8)	1.640 (8)
T(2)–O(5)	1.638 (9)	1.670 (8)	1.656 (8)	1.679 (8)
T(2)–O(6)	1.607 (9)	1.641 (10)	1.631 (8)	1.660 (8)
Average	1.615	1.647	1.626	1.666
O–O distances (Å)				
T(1) Tetrahedron				
O(1)–O(5)	2.701 (11)	2.704 (12)	2.696 (10)	2.715 (10)
O(1)–O(6)	2.728 (11)	2.699 (13)	2.724 (11)	2.725 (11)
O(1)–O(7)	2.697 (12)	2.703 (14)	2.712 (12)	2.743 (11)
O(5)–O(6)	2.677 (12)	2.713 (13)	2.683 (11)	2.749 (11)
O(5)–O(7)	2.700 (9)	2.696 (8)	2.700 (8)	2.725 (8)
O(6)–O(7)	2.664 (10)	2.709 (14)	2.666 (11)	2.736 (11)
Average	2.694	2.704	2.697	2.732
T(2) Tetrahedron				
O(2)–O(4)	2.747 (11)	2.769 (10)	2.750 (10)	2.816 (10)
O(2)–O(5)	2.683 (12)	2.673 (11)	2.673 (10)	2.691 (10)
O(2)–O(6)	2.641 (12)	2.654 (12)	2.644 (11)	2.700 (11)
O(4)–O(5)	2.460 (12)	2.706 (11)	2.495 (11)	2.727 (11)
O(4)–O(6)	2.643 (11)	2.586 (12)	2.690 (11)	2.608 (10)
O(5)–O(6)	2.633 (12)	2.753 (13)	2.661 (11)	2.775 (11)
Average	2.634	2.690	2.652	2.720
Si–Si distances (Å)				
T(1)–*T*(2) [through O(6)]	3.040 (5)	3.041 (5)	3.067 (4)	3.056 (4)
T(1)–*T*(2) [through O(5)]	3.050 (5)	3.001 (5)	3.055 (4)	3.024 (4)
T(1)–*T*(1) (across mirror)	3.080 (4)	3.032 (4)	3.116 (4)	3.063 (4)

TABLE 6. INTERATOMIC ANGLES (°) IN TETRAHEDRAL CHAINS FOR TWO ORTHOAMPHIBOLES

Atoms	Gedrite 001		Gedrite 002	
	A-Chain	*B*-Chain	*A*-Chain	*B*-Chain
O(1)–*T*(1)–O(5)	108.6 (4)	108.8 (4)	108.8 (4)	107.9 (4)
O(1)–*T*(1)–O(6)	112.2 (4)	108.7 (5)	111.5 (4)	108.9 (4)
O(1)–*T*(1)–O(7)	110.0 (5)	109.5 (6)	110.3 (5)	110.1 (5)
O(5)–*T*(1)–O(6)	108.0 (4)	110.0 (4)	108.7 (4)	110.5 (4)
O(5)–*T*(1)–O(7)	109.2 (5)	109.4 (5)	109.3 (5)	109.2 (5)
O(6)–*T*(1)–O(7)	108.8 (5)	110.5 (6)	108.2 (5)	110.2 (5)
O(2)–*T*(2)–O(4)	117.3 (5)	115.2 (4)	117.3 (4)	115.8 (4)
O(2)–*T*(2)–O(5)	110.0 (5)	107.2 (4)	109.6 (4)	106.3 (4)
O(2)–*T*(2)–O(6)	109.0 (4)	107.5 (5)	109.0 (4)	107.6 (4)
O(4)–*T*(2)–O(5)	99.6 (4)	110.1 (4)	99.8 (4)	110.5 (4)
O(4)–*T*(2)–O(6)	112.0 (4)	104.4 (5)	112.4 (4)	104.4 (4)
O(5)–*T*(2)–O(6)	108.4 (4)	112.5 (5)	108.0 (4)	112.4 (4)
T(1)–O(5)–*T*(2)	134.2 (6)	128.7 (5)	134.2 (5)	128.6 (5)
T(1)–O(6)–*T*(2)	139.3 (5)	134.8 (6)	139.2 (5)	133.3 (5)
T(1)–O(7)–*T*(1)	139.8 (8)	134.6 (9)	141.7 (8)	133.6 (7)
O(5)–O(6)–O(5)	162.4 (4)	147.5 (4)	162.5 (4)	146.0 (4)
O(5)–O(7)–O(6) Across mirror	164.0 (5)	146.8 (6)	163.9 (5)	145.4 (4)

complete *O*- or *S*-rotations will have O(5)–O(6)–O(5) angles of 120° and the hexads of tetrahedra will possess 3-fold symmetry (Fig. 1). Such rotations with O(5)–O(6)–O(5) angles of 120° correspond to maximum kinking of the tetrahedral chains and will be defined as *complete O*- or *S*-rotations. The O(5)–O(6)–O(5) angle in structures with incomplete rotations will lie in the range (120°, 180°].

Taking into account these possible rotations and defining an octahedral strip direction we can construct a set of schematic diagrams depicting the various amphibole structure types. The octahedral strip direction is defined by specifying the orientation of the octahedra with respect to the crystallographic axes (conventional right-handed orientation). One pair of octahedral faces of each octahedron lie parallel to the *b*-*c* plane; the upper and lower triangular faces of each octahedron are oriented in opposite senses, but all faces on the same side of an octahedral strip are oriented identically, We define a *positively* (+) directed strip as one in which the *lower* triangular faces of a given octahedral strip (as

TABLE 7. INTERATOMIC DISTANCES BETWEEN OXYGEN ATOMS *A*- AND *M*-SITE OCCUPANTS

Atoms	Gedrite 001				Gedrite 002			
	Site occupancy	Bond multiplicity	Distance *A*-set	*B*-set	Site occupancy	Bond multiplicity	Distance *A*-Set	*B*-set
A–O(6)	Na, 0.34 (3)	2	2.65 (2)	2.64 (2)	Na, 0.52 (3)	2	2.64 (1)	2.64 (1)
A–O(7)	Vacant, 0.66	1	2.41 (3)	2.30 (3)	vacant, 0.48	1	2.40 (2)	2.35 (2)
Mean for 6			2.55				2.54	
M(1)–O(1)	Fe*, 0.12 (1)	1	2.067 (9)	2.054 (10)	Fe*, 0.33 (1)	1	2.059 (8)	2.057 (8)
M(1)–O(2)	Mg, 0.88	1	2.130(9)	2.158 (8)	Mg, 0.67	1	2.165 (8)	2.156 (8)
M(1)–O(3)		1	2.078 (9)	2.061 (8)		1	2.101 (8)	2.068 (8)
Mean for 6			2.091				2.101	
M(2)–O(1)	Fe*, 0.04 (1)	1	2.028 (8)	2.005 (9)	Fe*, 0.09(1)	1	2.017 (8)	2.004 (8)
M(2)–O(2)	Mg, 0.36	1	1.985 (10)	2.021 (8)	Mg, 0.23	1	1.993 (8)	1.993 (8)
M(2)–O(4)	Al, 0.60	1	1.924 (9)	1.951 (8)	Al, 0.68	1	1.920 (8)	1.947 (8)
Mean for 6			1.986				1.979	
M(3)–O(1)	Fe*, 0.10 (2)	2	2.055 (8)	2.097 (9)	Fe*, 0.39 (2)	2	2.107 (8)	2.119 (8)
M(3)–O(3)	Mg, 0.90	1	2.017 (15)	2.023 (13)	Mg, 0.61	1	2.068 (12)	2.061 (12)
Mean for 6			2.057				2.097	
M(4)–O(2)	Fe*, 0.42	1	2.217 (9)	2.103 (8)	Fe*, 0.65	1	2.254 (8)	2.121 (8)
M(4)–O(4)	Mg, 0.55	1	2.123 (9)	2.015 (9)	Mg, 0.32	1	2.129 (8)	2.019 (8)
M(4)–O(5)	Ca, 0.02	1	2.222 (9)	2.416 (8)	Ca, 0.02	1	2.246 (7)	2.391 (8)
	Na, 0.01				Na, 0.01			
Mean for 6			2.183				2.193	
			z	(1−*z*)			*z*	(1−*z*)
M(1)–*M*(1)			3.154 (4)				3.197 (3)	
M(1)–*M*(2)			3.043 (6)	3.059 (6)			3.073 (4)	3.068 (4)
M(1)–*M*(3)			3.066 (6)	3.053 (6)			3.087 (4)	3.086 (4)
M(1)–*M*(4)			3.114 (4)				3.132 (3)	
M(2)–*M*(3)			3.135 (3)				3.165 (3)	
M(2)–*M*(4)			3.013 (5)	3.087 (5)			3.036 (4)	3.104 (4)

Fe* = Fe+Mn+Ti.

TABLE 8. SELECTED INTERATOMIC ANGLES (DEGREES) IN $M(1)$, $M(2)$, $M(3)$, $M(4)$, AND A SITES FOR TWO ORTHOAMPHIBOLES

Atoms	Bond angle multiplicity	Angle		Atoms	Bond angle multiplicity	Angle	
		Gedrite 001	Gedrite 002			Gedrite 001	Gedrite 002
O(1B)-$M(1)$-O(2B)	1	96.5 (3)	97.3 (3)	O(1B)-$M(3)$-O(1B)	1	101.4 (4)	103.2 (3)
O(1A)-$M(1)$-O(2A)	1	97.5 (4)	97.4 (3)	O(1A)-$M(3)$-O(1A)	1	101.4 (4)	102.0 (3)
O(1B)-$M(1)$-O(2A)	1	81.3 (4)	80.4 (3)	O(1B)-$M(3)$-O(1A)	2	78.6 (3)	77.4 (3)
O(1A)-$M(1)$-O(2B)	1	82.3 (3)	80.9 (3)	O(1B)-$M(3)$-O(3B)	2	95.9 (4)	96.7 (3)
O(1B)-$M(1)$-O(3B)	1	98.1 (4)	98.1 (4)	O(1A)-$M(3)$-O(3A)	2	95.5 (4)	95.8 (3)
O(1A)-$M(1)$-O(3A)	1	97.6 (4)	97.0 (4)	O(1B)-$M(3)$-O(3A)	2	84.1 (4)	84.2 (3)
O(1B)-$M(1)$-O(3A)	1	83.7 (5)	84.9 (4)	O(1A)-$M(3)$-O(3B)	2	84.5 (3)	83.3 (3)
O(1A)-$M(1)$-O(3B)	1	83.2 (4)	84.3 (4)				
O(2A)-$M(1)$-O(2B)	1	87.7 (3)	88.5 (3)	O(2B)-$M(4)$-O(2A)	1	86.9 (3)	87.1 (3)
O(3A)-$M(1)$-O(3B)	1	80.8 (4)	79.8 (3)	O(2B)-$M(4)$-O(4A)	1	81.0 (3)	79.2 (3)
O(2B)-$M(1)$-O(3B)	1	95.4 (4)	96.2 (3)	O(2B)-$M(4)$-O(4B)	1	95.0 (3)	96.5 (3)
O(2A)-$M(1)$-O(3A)	1	96.0 (4)	95.4 (3)	O(2B)-$M(4)$-O(5B)	1	88.9 (3)	88.6 (3)
				O(2A)-$M(4)$-O(4B)	1	78.0 (3)	77.5 (3)
O(1A)-$M(2)$-O(1B)	1	81.4 (4)	82.1 (3)	O(2A)-$M(4)$-O(4A)	1	86.7 (3)	86.0 (3)
O(1B)-$M(2)$-O(2B)	1	92.2 (4)	92.8 (3)	O(2A)-$M(4)$-O(5A)	1	103.0 (3)	102.2 (3)
O(1A)-$M(2)$-O(2A)	1	93.6 (4)	93.5 (3)	O(4A)-$M(4)$-O(5A)	1	68.9 (4)	69.4 (3)
O(1B)-$M(2)$-O(2A)	1	86.2 (4)	86.0 (3)	O(4A)-$M(4)$-O(5B)	1	85.2 (3)	85.9 (3)
O(1A)-$M(2)$-O(2B)	1	86.7 (3)	86.0 (3)	O(4B)-$M(4)$-O(5A)	1	117.3 (3)	117.1 (3)
O(1B)-$M(2)$-O(4B)	1	93.9 (4)	93.7 (3)	O(4B)-$M(4)$-O(5B)	1	109.9 (3)	110.3 (3)
O(1A)-$M(2)$-O(4A)	1	90.4 (4)	89.5 (3)	O(5B)-$M(4)$-O(5A)	1	76.8 (3)	77.5 (3)
O(2B)-$M(2)$-O(4B)	1	94.1 (4)	94.6 (3)				
O(2A)-$M(2)$-O(4A)	1	93.5 (4)	93.6 (3)	O(7A)-A-O(6B)	2	86.3 (7)	88.0 (5)
O(2B)-$M(2)$-O(4A)	1	88.1 (4)	87.6 (3)	O(7A)-A-O(6A)	2	63.2 (5)	63.5 (4)
O(2A)-$M(2)$-O(4B)	1	85.4 (4)	85.8 (3)	O(7B)-A-O(6B)	2	99.4 (8)	97.9 (5)
O(4A)-$M(2)$-O(4B)	1	94.2 (4)	94.7 (3)	O(7B)-A-O(6A)	2	112.8 (7)	112.5 (4)
				O(6B)-A-O(6A)	2	77.6 (4)	73.3 (3)
				O(6B)-A-O(6B)	1	89.8 (8)	89.8 (5)
				O(6A)-A-O(6A)	1	104.9 (8)	105.4 (5)

viewed looking perpendicular to the b-c plane and along $-a^*$) have one of their three apices pointing in the $+c$ direction. If these lower faces have one of their apices pointing in the $-c$ direction, the strip is said to be negatively (−) directed. The orientations of the octahedral strips in the four amphibole polymorphs may be visualized with the aid of Figure 3. All (+) directed octahedral strips have one apex of the lower triangular faces directed away from the reader's eye (along +c); the negatively (−) directed strips have lower triangular faces oriented with one apex pointed toward the reader's eye (along $-c$).

Orthoamphiboles and $P2_1/m$ clinoamphiboles have two symmetrically distinct tetrahedral chains which we designate A and B, whereas $C2/m$ clinoamphiboles and protoamphiboles have only one kind of tetrahedral chain. The structures of these four amphibole "polymorphs" are diagrammatically presented as "I-beam" diagrams in Figure 3. The octahedral strip is shown in the center of the "I-beam" and is articulated

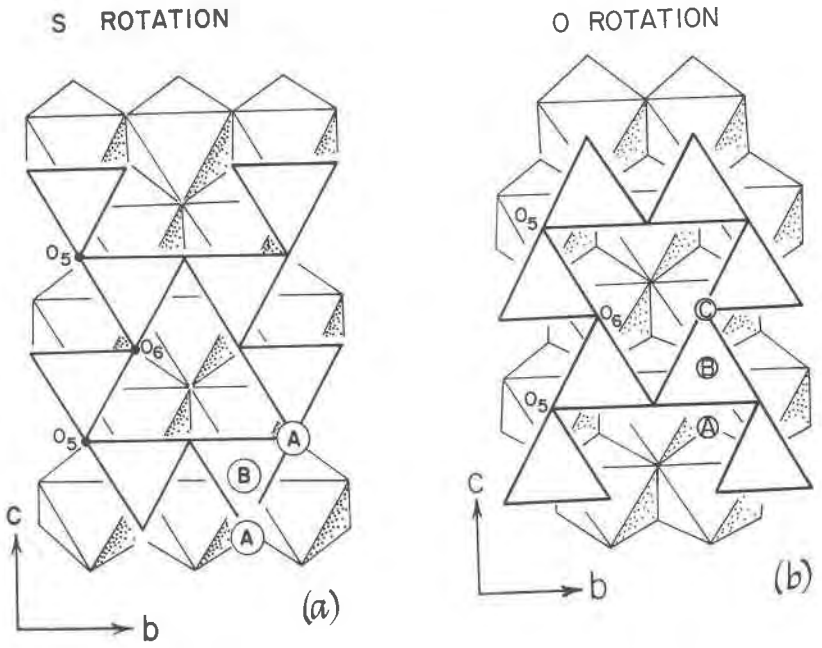

FIG. 1. A portion of the idealized orthoamphibole structure projected on to the *b-c* plane, tetrahedral strip above, octahedral strip below. (a). illustrates a *complete* *S*-tetrahedral rotation. (b). illustrates a *complete* *O*-tetrahedral rotation.

above and below by tetrahedral chains. The orientation of the "I-beams" (+) or (−) is defined in terms of the orientation of the octahedral strips as discussed above. The simplest of these "I-beam" diagrams is that of the *C*2/*m* clinoamphiboles such as tremolite and *C*-centered cummingtonite. This *C*2/*m* structure-type is made up of "I-beams" containing only *O*-rotations and the beams are stacked in the sequence (+,+,+,+). Protoamphibole (space group *Pnmn*, Gibbs, 1969) is also made up of "I-beams" containing only *O*-rotations. However, these "I-beams" are stacked in the sequence (+,−,+,−).

Orthoamphiboles (space group *Pnma*) are made up of "I-beams" having *O*-rotations and the stacking sequence of the beams is (+,+,−,−). The gedrite crystal structures possess incomplete *O*-rotations with *O*-rotations of 147.5° and 146.0° in the *B*-chains and of 162.4° and 162.5° in the *A*-chains for gedrites 001 and 002, respectively (Table 6). These angles show that the complete *O*-rotation is more nearly achieved in the *B*-chains than the A-chains. In any case, the drawing of the ideal gedrite structure (Fig. 2) predicts that both the *M*(4) site and the *A*-site will

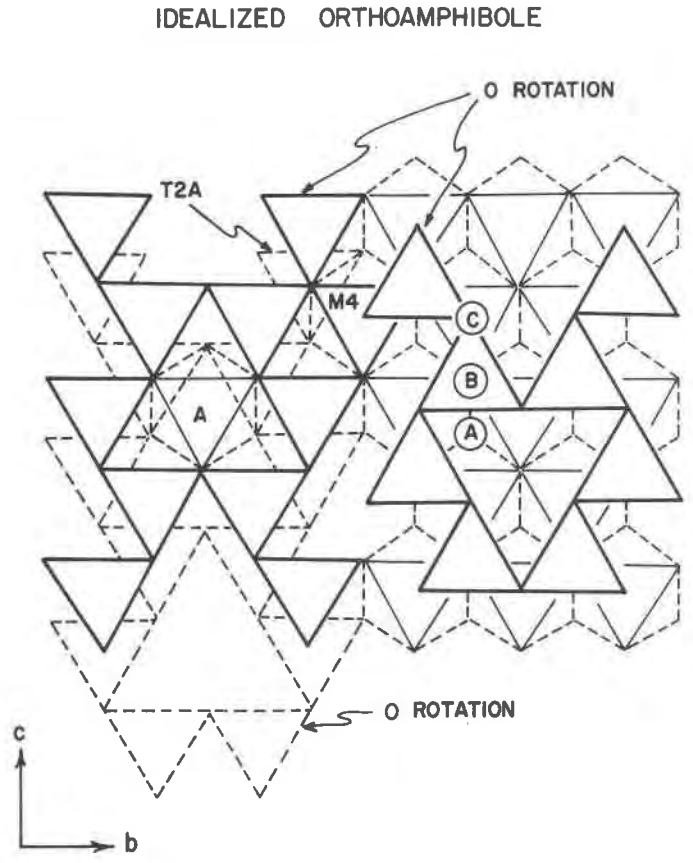

FIG. 2. A diagram of an idealized orthoamphibole structure showing O-rotations, octahedral $M(4)$ and A-sites, and polyhedral edge sharing.

become octahedral, that an $M(4)$-octahedron will share one edge with a tetrahedron and that the A-octahedron will share two edges with two tetrahedra. All of these predictions are realized in the real structure (Fig. 4) and the implications with regard to intracrystalline cation distributions are discussed later. Additional features of gedrite topology are illustrated in Figure 5.

The crystal structure of a $P2_1/m$ manganoan cummingtonite from Gouverneur, New York is given by Papike, Ross, and Clark (1969). This clinoamphibole is similar to the orthoamphibole in that both A- and B-type chains are present. On the other hand, the "I-beam" stacking sequence (+,+,+,+) is identical to that of the $C2/m$ polymorph (Fig. 3).

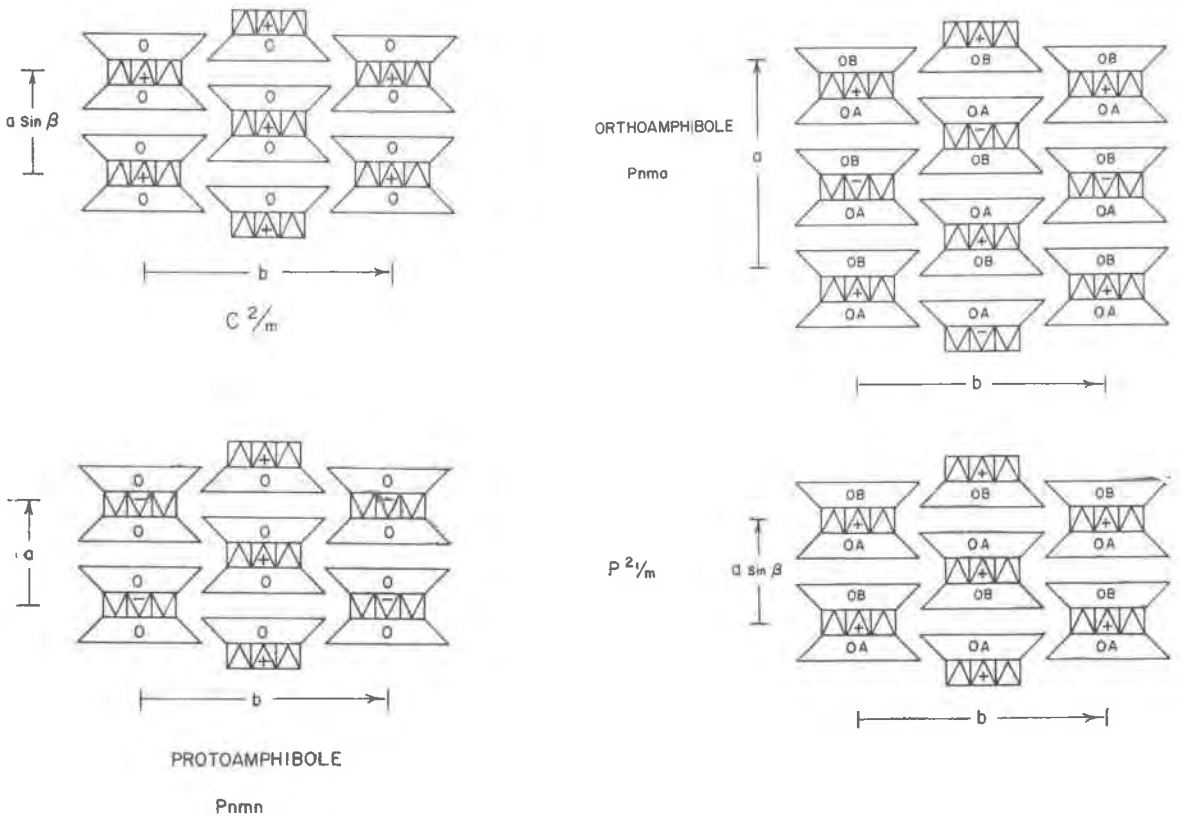

Fig. 3. "I-beam" diagrams for comparison of $C2/m$, *Pnmn*, *Pnma*, and $P2_1/m$ structure topologies. Definition of *O*-rotations is based rigorously on the proposals of Thompson (1970)

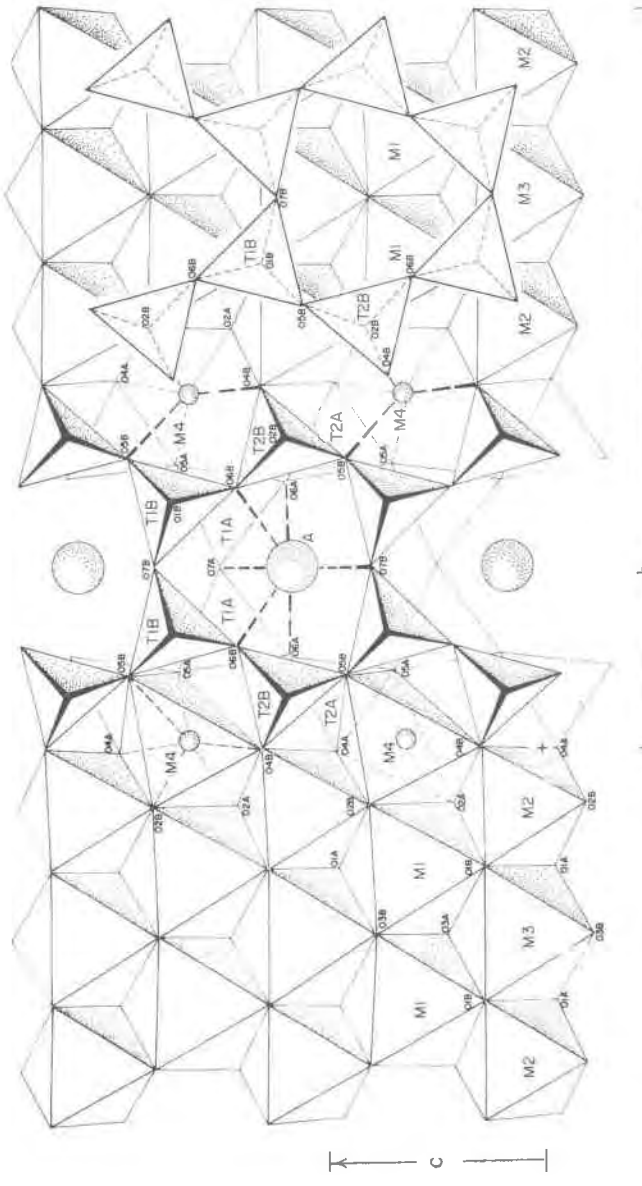

Fig. 4. Diagram of the *Pnma* gedrite structure viewed along *a*, showing selected portions of the unit cell contents.

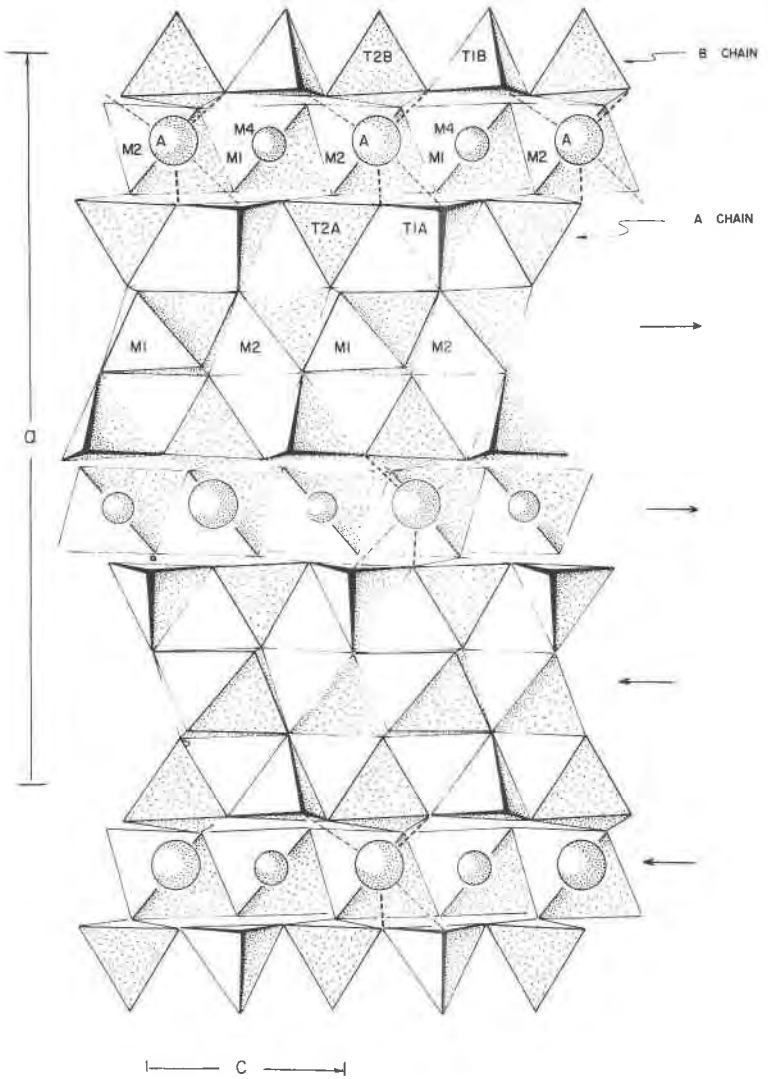

FIG. 5. Diagram of the *Pnma* gedrite structure viewed along *b*, showing selected portions of the unit cell contents.

The $P2_1/m$ clinoamphibole has *A*- and *B*-chain *O*-rotations of 178.4° and 166.2°, respectively.

It is of interest to compare the "real" structure topologies of the amphiboles described above with the "ideal" topologies of Thompson's (1970) rotated structures. Several significant differences are apparent.

First, only *O*-rotations have been found in the real structures and second, Thompson's parity rule is violated in protoamphibole and in the A layers of orthoamphibole. Thompson's statement of the parity rule is as follows: "This rule derives from the regularity of the polyhdera and affects the nature of the rotations of adjacent tetrahedral strips in a given tetrahedral layer. If two such tetrahedral strips are both rotated in the same sense then the two octahedral strips (one above and one below the tetrahedral layer) to which they are joined across (100) must both have a 'tilt' or 'skew'[1] of the same sense. If the rotations are in opposite senses then the tilts must be in opposite senses." The necessity for this parity rule for completely rotated structures is illustrated diagrammatically in Figure 6. It is apparent that the I-beams in Fig. 6C, which violate the rule cannot be fitted together. Based on this rule we would predict the occurrence of both *O*- and *S*-rotations in the protoamphibole and orthoamphibole structures since two different "skews" of the octahedral layer exist. Figure 7 illustrates how the "real" gedrite structure is put together in violation of the parity rule. This rule was derived for closest packed oxygen structures with completely rotated chains (O(5)–O(6)–O(5) = 120°) and regular polyhedra. In the "real" structure (Figure 7) linkage between tetrahedral and octahedral layers is achieved in violation of the parity rule by extention of the *A*-chain (O(5)–O(6)–O(5) angles = 162.4° and 162.5°) and distortion of the polyhedra (especially the $M(2)$ site). In summary it may be stated that "real" amphibole structures show a strong preference for *O*-rotations in agreement with Thompson's (1970) prediction.

Crystal Chemical Aspects of Gedrite Structures

Now that the general topologic features of the gedrite structures have been discussed we may consider the distribution of cations over the crystallographically distinct sites. We will concern ourselves with the "crystal-chemical components", Na, Mg, Al, Si, Fe*, and vacancies. Fe* refers to Fe^{2+}, Fe^{3+}, Mn and Ti which cannot be readily distinguished by the X-ray method. The chemical analyses (Table 1) indicate that this is not a bad approximation since most of Fe* is Fe^{2+}. The three main cation distribution problems in gedrites are first; the vacancy versus Na content of the *A*-sites, second; the distribution of Fe*, Mg, and Al over the $M(1)$, $M(2)$, $M(3)$, and $M(4)$ sites, and third; the distribution of Al and Si over the $T(1A)$, $T(1B)$, $T(2A)$, and $T(2B)$ sites.

The A-Site. The occupants of the *A*-site in gedrite (Figure 4) are more

[1] Thompson's definition of "skew" or "tilt" is directly analogous to our definition of plus and minus octahedral strip directions.

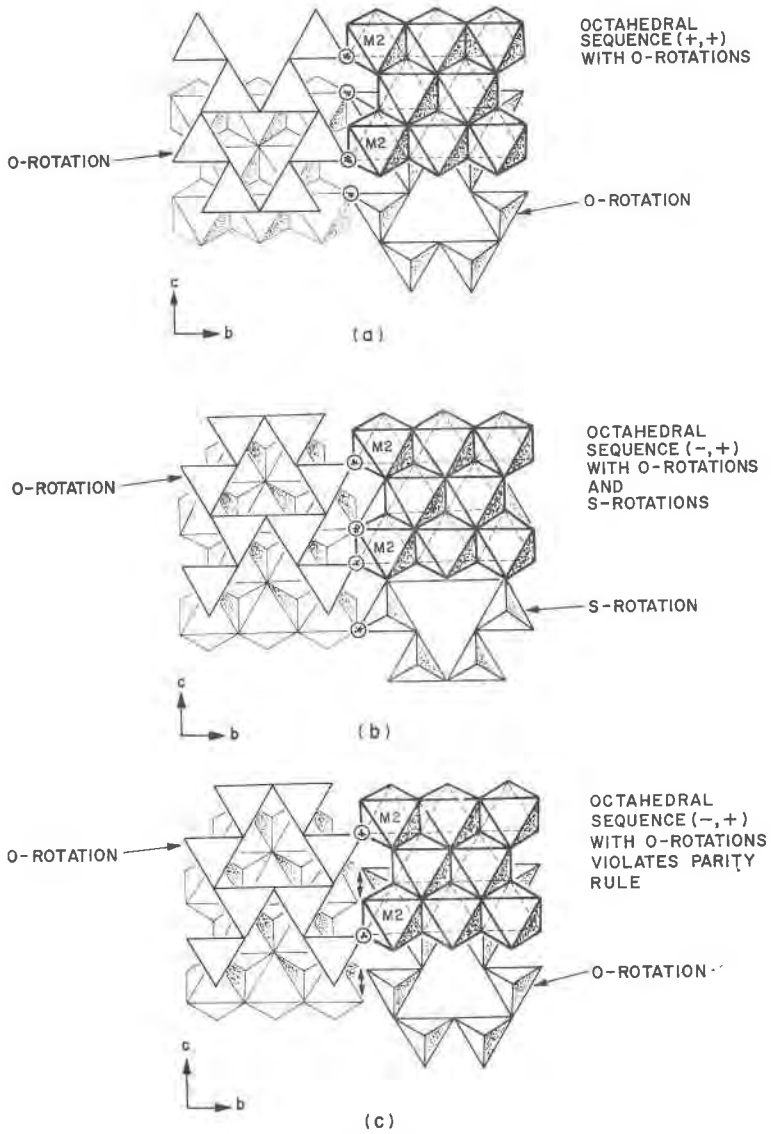

FIG. 6. Geometrical stacking possibilities for "Ideal" completely rotated amphibole structures after Thompson (1970). Figure 6c illustrates violation of parity and the doubly pointed arrows show the degree of mismatch between tetrahedra and octahedra.

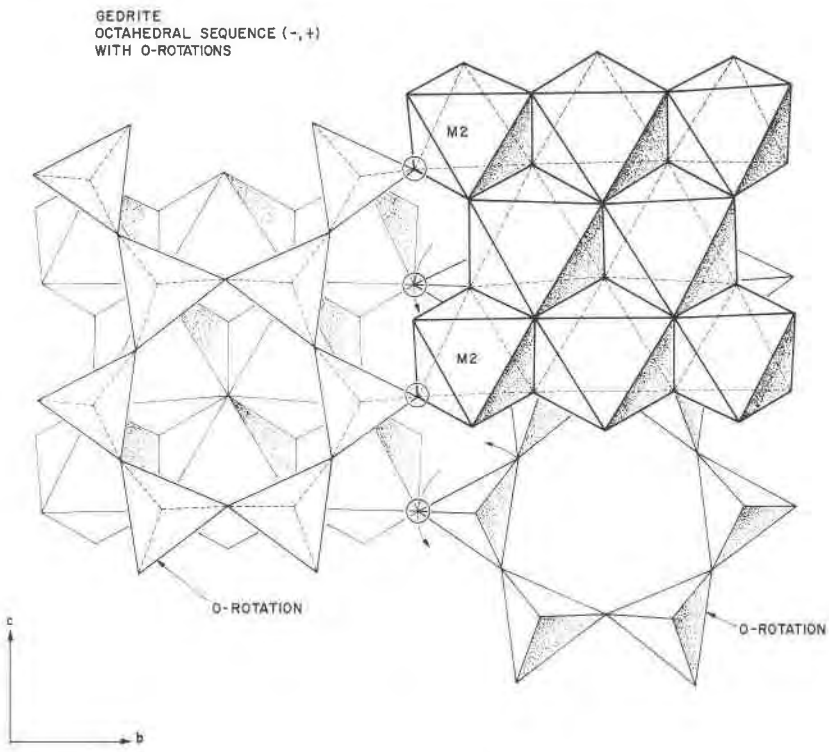

FIG. 7. Portion of the "Real" gedrite structure showing how the tetrahedral chain-octahedral chain linkage is achieved in violation of Thompson's (1970) parity rule. The A-chains (illustrated) rotate and extend to reduce the effect of the violation.

tightly coordinated than the A-site atoms in $C2/m$ amphiboles. In $C2/m$ amphiboles the tetrahedral chains above and below the site are oppositely directed and the atoms in the site show a high degree of positional disorder. On the basis of a split atom model one can consider the site in $C2/m$ amphiboles as essentially eight coordinated (Papike, Ross and Clark, 1969). In gedrites the tetrahedral chains above and below the A-site are identically directed. This leads to an essentially six-coordinated site in gedrites and the Na in this site displays less positional disorder than in $C2/m$ amphiboles. The identical direction of the tetrahedral chains above and below the A-site (Figures 2 and 4) in orthoamphiboles results from first; the fact that the octahedral strips on either side of the A-site have different "skews", *i.e.* one is plus and the other is minus and second; that both the A- and B-tetrahedral chains have O-rotations. The orientations of the A- and B-chains are illustrated in Figure 8. Note that

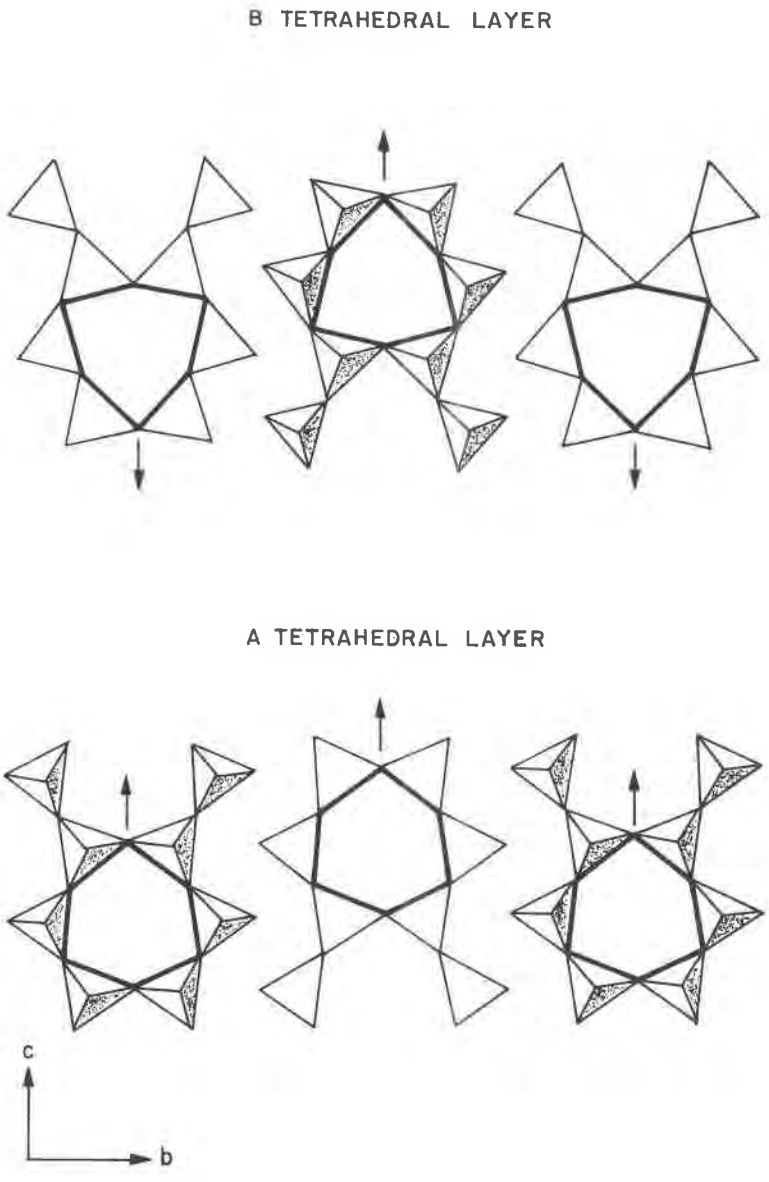

FIG. 8. Orientation of tetrahedral chains in *A*- and *B*-layers of the "Real" gedrite structure.

TABLE 9. SITE OCCUPANCIES FOR M- AND A-SITES

Site		Anthophyllite (Finger 1970a,b)	Gedrite 001 Present Study	Gedrite 002 Present Study
	Atom		*Mole Fraction*	
$M(1)$	Mg	0.96	0.88	0.67
	Fe*	0.04	0.12	0.33
$M(2)$	Al	—	0.60	0.68
	Mg	0.97	0.36	0.23
	Fe*	0.03	0.04	0.09
$M(3)$	Mg	0.97	0.90	0.61
	Fe*	0.03	0.10	0.39
$M(4)$	Mg	0.35	0.55	0.32
	Fe*	0.65	0.42	0.65
	Ca	—	0.02	0.02
	Na	—	0.01	0.01
A	Na	—	0.34	0.52
	Vacant	1.00	0.66	0.48

* $Fe^* = Fe^{2+} + Fe^{3+} + Mn + Ti$.

in the B-tetrahedral layers adjacent tetrahedral chains are oriented in opposite directions, *i.e.* the trigonal aspect or "arrowheads" of the six-membered rings reverse. Adjacent chains in the B-layers are related by 2_1 axes parallel to b. In the A-tetrahedral layers, however, adjacent tetrahedral layers are identically directed, *i.e.*, all "arrowheads" point in the same direction. Adjacent chains in the A-layers are related by 2_1 axes parallel to c. It is also interesting to note that the A-tetrahedral layers (identically oriented "arrowheads") are sandwiched between octahedral layers with reversed "skews" whereas B-tetrahedral layers are between octahedral layers of the same "skews". The A-tetrahedral chain is the one involved in the parity violation and is more nearly extended than the B chain, which tends to reduce the degree of violation.

We used the least squares method of Finger (1969 b) to obtain the Na content of the A-site (Table 9). The result of this refinement agrees very well with the predicted A-site occupancy based on the analyses of gedrite 002 (predicted; 0.53 Na; observed; 0.52Na) but not so well for gedrite 001 (predicted 0.45 Na, observed; 0.34) (Tables 7, 9). However, the formula of gedrite 001 is based on an electron microprobe analysis and is subject to the limitations of formulas calculated from such analyses. There is good evidence based on temperature-factor measurements that

the Na content in the A-site of gedrite 001 determined by the site occupancy method is correct. Since, if we first assume the formula calculated from the analysis is correct and assign (0.45) Na to the A-site the isotropic temperature factor is approximately 2.5 (Å^2), an unusually high value for silicate structures. However, if we refine the occupancy, the Na content drops immediately to (0.34) and the isotropic temperature factor drops to 1.47 (Å^2), which is nearly identical to the isotropic temperature factor for Na, 1.53 (Å^2), in the A-site of gedrite 002.

The M-Sites. The determination of the site occupancies for the M-sites was done in the following way. First, small amounts of Na and Ca were assigned to the $M(4)$ site to bring the total number of cations in the M-sites up to seven. Next, the mean metal-oxygen distance for the $M(2)$ site was significantly smaller than for $M(1)$, $M(3)$, or $M(4)$ (Table 7) and was consistent with an essentially ordered octahedral aluminum content in this site. Thus, after assigning all the octahedral aluminum to the $M(2)$ site we could refine Fe* against Mg for the unfilled portion of the $M(2)$ site and for the $M(1)$, $M(3)$, and $M(4)$ sites (Finger, 1969b). The results are given in Tables 7 and 9.

The T-Sites. The site occupancies for the T-sites were estimated using mean $(T-O)$ distance arguments similar to those proposed by Smith (1954) and Smith and Bailey (1963). The specific method used for the gedrites was method number (2) suggested by Papike, Ross, and Clark (1969) where the mean $(T-O)$ distance for each site containing Al is compared to an equivalent site in an amphibole that contains only silicon. In our case, we compared the mean $(T-O)$ distances for gedrites with those for anthophyllite (Finger, 1970b) (Table 10). The increase in mean $(T-O)$ distance compared with anthophyllite plus a knowledge of the tetrahedral Si:Al ratio from the analyses enables us to make some estimates of the occupancies for each site (Table 11).

Discussion

Polymorphism in Amphiboles. Refinement of the orthoamphibole structures enables us to compare orthoamphiboles, $P2_1/m$ amphiboles, and $C2/m$ amphiboles and to consider the general problem of polymorphism in the low-calcium region of the amphibole quadrilateral (Ross, Papike, and Weiblen, 1968). We have pointed out the topologic similarities between $C2/m$, $P2_1/m$, *Pnma* amphiboles. It is also of interest to compare the coordination of the $M(4)$ site in these amphiboles. In the orthoamphiboles the $M(4)$ site is six-coordinated, with a mean $(M-O)$ distance of approximately 2.19 Å (Table 7). In $C2/m$ cummingtonite

TABLE 10. COMPARISON OF T–O DISTANCES FOR THREE ORTHOAMPHIBOLES

Atoms	Anthophyllite Finger (1970b)	Gedrite 001 Present study	Gedrite 002 Present study
T(1A)–O(1A)	1.618	1.651	1.653
–O(5A)	1.640	1.673	1.660
–O(6A)	1.611	1.635	1.641
–O(7A)	1.615	1.640	1.649
Mean	1.621	1.650	1.651
$\Delta(T$–O)	—	+0.029	+0.030
T(2B)–O(1B)	1.618	1.665	1.679
–O(5B)	1.636	1.658	1.677
–O(6B)	1.622	1.654	1.668
–O(7B)	1.617	1.643	1.666
Mean	1.623	1.655	1.672
$\Delta(T$–O)	—	+0.032	+0.049
T(2A)–O(2A)	1.619	1.635	1.613
–O(4A)	1.601	1.579	1.605
–O(5A)	1.655	1.638	1.656
–O(6A)	1.621	1.607	1.631
Mean	1.624	1.615	1.626
$\Delta(T$–O)	—	−0.009	+0.002
T(2B)O–(2B)	1.630	1.648	1.683
–(4B)	1.608	1.630	1.640
–(5B)	1.643	1.670	1.679
–(6B)	1.653	1.641	1.660
Mean	1.634	1.647	1.666
$\Delta(T$–O)	—	+0.013	+0.032

(Ghose, 1961), in grunerite (Finger, 1969a), and in $P2_1/m$ and in $C2/m$ cummingtonite (Papike, Ross, and Clark, 1969) the mean $M(4)$-O distance is 2.30 Å. In fact, the $M(4)$ site in the Mg-Fe^{2+} clinoamphiboles can be considered essentially four-coordinated with the four shortest $M(4)$—O bonds equal to approximately 2.12 Å. It is fair to say, therefore, that the $M(4)$ coordination in orthoamphiboles is tighter than in clinoamphiboles of the same composition. This, in fact, probably explains

why the molar volumes for anthophyllites are lower than for $C2/m$ cummingtonites of equivalent compositions (Finger, 1967, 1970b).

There is good chemical evidence that the composition fields of $C2/m$ cummingtonite, $P2_1/m$ cummingtonite, and anthophyllite overlap and it was suggested by Ross, Papike, and Shaw (1969, p. 294) that the $P2_1/m$ phase is a metastable intermediate. Prewitt, Papike, and Ross (1970) found in heating experiments that the $P2_1/m$ manganoan cummingtonite inverts reversibly to the $C2/m$ structure-type. These considerations, coupled with our new knowledge of the orthoamphibole structure suggest the following relationships between the amphibole polymorphs. At high temperatures a $C2/m$ cummingtonite is stable. On cooling,

TABLE 11. DISTRIBUTION OF TETRAHEDRAL ALUMINUM IN GEDRITES

	Gedrite 001	Gedrite 002
	X_{Al}	
T(1A)	0.34	0.27
T(1B)	0.38	.44
T(2A)	0.00	.02
T(2B)	0.16	.29

the orthoamphibole stability field is entered and recrystallization to the *Pnma* structure should occur. Such an inversion, however, involves not only further kinking of the tetrahedral chains, but more importantly involves a change in the stacking sequence of the "I-beams" from (+,+,+,+) to (+,+,−,−); the latter requiring the breaking of major chemical bonds. Such a reconstructive transformation may not be possible unless a fluid phase is present, or it may be prevented by "structural control" of the primary $C2/m$ cummingtonite. If this reconstructive transformation is prevented, a metastable $P2_1/m$ cummingtonite may form from the $C2/m$ phase by a simple displacive transformation which requires no breaking of chemical bonds. Such a transformation would particularly involve a change in the degree of tetrahedral chain rotation. It is certainly not proven that the $P2_1/m$ clinoamphibole is a metastable phase, but considering the apparent composition overlap with $C2/m$ cummingtonite and anthophyllite, if stable its field of stability must be very small.

Fe-Mg Distributions in Orthoamphiboles. The Fe*-Mg distributions for three orthoamphiboles are summarized in Table 9. Anthophyllite (Finger, 1970b) is highly ordered, and if the distribution isotherms for

TABLE 12. Fe*-Mg DISTRIBUTIONS IN ORTHOAMPHIBOLE M-SITE[a]

	Anthophyllite Finger (1970)	Gedrite 001 Present Study	Gedrite 002 Present Study
$M(1)$	0.04	0.12	0.33
$M(2)$	0.03	0.10	0.28
$M(3)$	0.03	0.10	0.39
Weighted mean[b]	0.03	0.11	0.32
$M(4)$	0.65	0.43	0.67
K_D	0.019	0.164	0.232

[a] Fe*-Mg distributions are given in terms of Fe*/Fe*+Mg ratios for that portion of the site not occupied by aluminum. Fe* = $Fe^{2+}+Fe^{3+}+Ti+Mn$.

[b] The Fe*/Fe*+Mg ratios are weighted according to the site multiplicities for $M(1)$, $M(2)$, and $M(3)$.

orthopyroxenes (Virgo and Hafner, 1969) are at all applicable to orthoamphiboles a relatively low temperature of Mg-Fe* ordering is indicated. Direct comparison of the Fe*-Mg distributions in the gedrites with anthophyllites is confused by the fact that the $M(2)$ octahedra of gedrites are enriched in aluminum. Therefore, to facilitate comparison we have recast the analyses in the form of Fe*/Fe*+Mg ratios (Table 12). When this is done we see that there is no appreciable fractionation of Fe* and Mg between the $M(1)$, $M(2)$, and $M(3)$ sites of anthophyllite or gedrite 001, but the $M(2)$ site of gedrite 002 appears slightly depleted in Fe* relative to $M(1)$ and $M(3)$.

We may consider the following exchange reaction for orthoamphiboles.

$$\text{Fe*}(4) + \text{Mg}(1, 2, 3) \rightleftarrows \text{Mg}(4) + \text{Fe*}(1, 2, 3)$$

where Fe*(4) refers to Fe* in the $M(4)$ site and Mg(1,2,3) refers to magnesium in the $M(1)$, $M(2)$ and $M(3)$ sites, etc. A distribution coefficient K_D can be defined for intracrystalline exchange between $M(4)$ and the mean of $M(1)$, $M(2)$, $M(3)$ as:

$$K_D = \frac{[1 - X(4)][X(1, 2, 3)]}{[X(4)][1 - X(1, 2, 3)]}$$

where $X(4)$ refers to the mole fraction of Fe* in the $M(4)$ site and $X(1,2,3)$ refers to the mean mole fraction of Fe* weighted according to site multiplicities for the portions of the $M(1)$, $M(2)$, and $M(3)$ sites that are not occupied by aluminum. The intracrystalline distribution coefficients calculated in this manner are 0.019 for anthophyllite, 0.164

for gedrite 001, and 0.232 for gedrite 002. Thus the sequence from most ordered to most disordered is anthophyllite, gedrite 001 and gedrite 002. However, the temperature implications of these distributions are less obvious. If ideal mixing of iron and magnesium on each of the M-sites (Mueller, 1962) is a good assumption (such is indicated for magnesium-rich orthopyroxenes: Virgo and Hafner, 1969) then it is probably valid to compare gedrite 001 and gedrite 002. The distribution coefficients would then indicate that the Fe*—Mg ordering of gedrite 002 reflects a higher temperature than gedrite 001. It is more difficult to compare the temperature significance of the gedrites with anthophyllite. The reason for this is that the ordering kinetics may be significantly different. In anthophyllite nearest M-site exchange of Fe and Mg between the $M(4)$ site and the $M(1)$ and $M(2)$ sites can be accomplished (Figure 4). However, in gedrite the $M(2)$ sites are largely blocked by aluminum which may significantly impede the ordering rates.

Si—Al Distributions in Gedrites. The Si—Al distributions for the two gedrites are summarized in Table 11. The most obvious feature of these distributions is that Al is distributed over the $T(1A)$, $T(1B)$, and $T(2B)$ but $T(2A)$ is largely occupied by silicon. There appears to be an obvious structural explanation for this. The $T(2A)$ tetrahedron and the $M(4)$ octahedron share an edge and as a result the $O(4A)$—$O(5A)$ distance is very short (2.460 Å, Table 5) and the tetrahedral site thus inherently small. This small tetrahedron naturally exhibits a strong site preference of silicon over aluminum.

The Gedrite-Anthophyllite Solvus. Evidence for the gedrite-anthophyllite solvus based on naturally occurring samples has been presented by Robinson, Jaffe, Klein, and Ross (1969), Stout (1969), Ross, Papike, and Shaw (1969), Robinson, Ross, and Jaffe (1970), and Stout (1970). Robinson *et al.* (1970) suggest that there is complete solid solution at high temperatures between anthophyllite $R_7^{2+}Si_8O_{22}(OH)_2$ and gedrite $Na_{0.5}R_2(R_{3.5}^{2+}R_{1.5}^{3+})Al_2Si_6O_{22}(OH)_2$. It is of interest to consider the sites that are involved in the exsolution reactions at lower temperatures. Based on the recent refinements of orthoamphiboles and the chemical studies mentioned above we can predict that phase separation of anthophyllite and gedrite from an anthophyllite-gedrite solid solution involves separation of Na and vacancies in the A-site, R^{3+} and R^{2+} in the $M(2)$ site, and Si and Al in the tetrahedral sites. The $M(4)$ site which plays such an important role in exsolution of calcic amphibole-(Fe^{2+},Mg) amphibole solid solutions (Ross, *et al*, 1969) plays a rather passive role in orthoamphibole exsolution.

Other Possible Structure Models for Gedrite. Thompson (1970) pointed out $P2_1ma$ as a possible space group for orthoamphibole structures. Although we have yet to find X-ray evidence for this space group it is possible that the *Pnma* structure reported here is an average structure comprised of ordered domains of $P2_1ma$ symmetry. In fact, if the structure did exhibit $P2_1ma$ symmetry, certain features of the chemistry could be more easily explained. As pointed out above, Robinson *et al.* (1970) have suggested that gedrite of composition $Na_{0.5}R_{5.5}^{2+}R_{1.5}^{3+}Si_6Al_2O_{22}(OH)_2$ may be an "end-member" of the anthophyllite-gedrite solid solution series. It is of interest to note that this formula can be arrived at by combining orthoamphibole components $R_5^{2+}R_2^{3+}Si_6Al_2O_{22}(OH)_2$ and $NaR_6^{2+}R^{3+}Si_6Al_2O_{22}(OH)_2$ in the ratio 1:1. In the first of these the A-site would be vacant and the $M(2)$ site would be filled with R^{3+}. In the second, the A-site would be filled with Na and the predicted $M(2)$ site occupancy would be $0.5R^{3+}$, $0.5R^{2+}$. In space group $P2_1ma$ we can have two symmetrically distinct "I-beams" arranged in stacks parallel to a and c with symmetrically distinct stacks alternating along b. It is interesting to speculate that ordered domains in gedrite might contain these two types of "I-beams", each type having the composition of one of the components mentioned above. The "end-member" gedrite $[Na_{0.5}R_{5.5}^{2+}R_{1.5}^{3+}Si_6Al_2O_{22}(OH)_2]$ could then be made up of the two compositionally distinct "I-beams" in the ratio 1:1.

Conclusions

In conclusion, the structure refinements of two gedrites have helped unravel the crystal-chemical complexity of this group of minerals. Specifically, we have identified two types of tetrahedral chains (A and B) with different degrees of O-rotation that lead to octahedral coordination of both the A and $M(4)$ sites. Polymorphism among *Pnma*, $P2_1/m$, and $C2/m$ Fe^{2+}—Mg amphiboles is more clearly understood when thought of in terms of these rotations. The sharing of polyhedral edges that results from these rotations has a pronounced effect on the distribution of Si and Al over the four crystallographically distinct tetrahedral sites. The tetrahedron which shares an edge with the $M(4)$ octahedron is largely occupied by silicon, and Al and Si are distributed over the remaining three. Gedrite-anthophyllite exsolution results from lack of mixing at low temperatures of Al and (Fe,Mg) on the $M(2)$ site, Al and Si on the tetrahedral sites, and Na and vacancies on the A-site. The $M(4)$ site plays a passive role in anthophyllite-gedrite exsolution compared to exsolution involving calcic-and calcium-poor clinoamphiboles. Although no X-ray evidence for space groups other than *Pnma*

was found for gedrite, it is conceivable that ordered domains with $P2_1ma$ symmetry exist within gedrite crystals. Ordered domains with this symmetry might explain the apparent "end-member" composition of the anthophyllite-gedrite solid solution series, $Na_{0.5}R_{5.5}^{2+}R_{1.5}^{3+}Si_6Al_2O_{22}(OH)_2$. Site occupancy refinements have demonstrated that octahedral aluminum is ordered in the $M(2)$ site and that Fe^{2+} and Mg are distributed over the $M(1)$, $M(2)$, $M(3)$, and $M(4)$ sites with Fe^{2+} showing a strong site preference for the $M(4)$ site. It is suggested that these Fe^{2+}–Mg distributions will be useful in determining thermal histories of gedrite-bearing rocks.

Acknowledgements

We gratefully acknowledge the help of A. T. Anderson, who did the electron microprobe analyses on gedrite 001, and Larry Finger, who furnished data on anthophyllite prior to publication. We also thank Joan R. Clark, J. B. Thompson, Jr., Larry Finger, Peter Robinson, D. E. Appleman, and C. T. Prewitt for stimulating discussions concerning this research, and Judith A. Konnert for help with computations.

The research was supported in part by a National Science Foundation Grant (No. GA-12973).

References

Bancroft, G. M., and R. G. J. Strens (1966) Cation distribution in anthophyllite from Mössbauer and infrared spectroscopy. *Nature*, **212**, 913–915.

Barker, F. (1961) Anthophyllite-biotite-hypersthene-rhodolite assemblage, Mason Mountain, North Carolina. *U. S. Geol. Surv. Prof. Pap.* **424C**, C336–C338.

Clark, J. R., D. E. Appleman, and J. J. Papike (1969) Crystal-chemical characterization of clinopyroxenes based on eight new structure refinements. *Mineral. Soc. Amer. Spec. Pap.* **2**, 31–50.

Cromer, D. T., and J. T. Waber (1965) Scattering factors computed from relativistic Dirac-Slater wave functions. *Acta Crystallogr.* **18**, 104–109.

Finger, L. W. (1967) *The Crystal Chemistry of Ferromagnesian Amphiboles*. Ph.D. Thesis, Department of Geology, U. of Minnesota.

——— (1969a) The crystal structure and cation distribution of a grunerite. *Mineral. Soc. Amer. Spec. Pap.* **2**, 95–100.

——— (1969b) Determination of cation distributions by least-squares refinement of single-crystal X-ray data. *Carnegie Inst. Year Book*, **67**, 216–217.

——— (1970a) The structure refinement and cation ordering of an anthophyllite [abstr.] *Amer. Mineral.* **55**, 300.

——— (1970b) Refinement of the crystal structure of an anthophyllite. *Carnegie Inst. Year Book*, **68**, 283–288.

Franzini, M. (1969) The A and B mica layers and the crystal structure of sheet silicates. *Contrib Mineral. Petrology*, **21**, 203–224.

———, and L. Schiaffino (1963) Polimorfismo e leggi de geminazione delle biotiti. *Atti Soc. Toscana Sci. Natur., Mem., A*, **70**, 60–98.

Ghose, S. (1961) The crystal structure of cummingtonite. *Acta Crystallogr.* **14**, 622–627.

Gibbs, G. V. (1969) Crystal structure of protoamphibole. *Mineral. Soc. Amer. Spec. Pap.* **2**, 101–109.

HEINRICH, E. W. (1950) Paragenesis of the rhodolite deposit, Masons Mountain, North Carolina. *Amer. Mineral.* **35,** 764–771.

HENDERSON, E. P. (1931) Notes on some minerals from the rhodolite quarry near Franklin, North Carolina. *Amer. Mineral.* **16,** 563–568.

MUELLER, R. F. (1962) Energetics of certain silicate solid solutions, *Geochim. Cosmochim. Acta* **26,** 581–598.

PAPIKE, J. J., M. ROSS, AND J. R. CLARK (1969) Crystal-chemical characterization of clinoamphiboles based on five new structure refinements. *Mineral. Soc. Amer. Spec. Pap.* **2,** 117–136.

PREWITT, C. T., J. J. PAPIKE, AND M. ROSS (1970) Cummingtonite: a reversible nonquenchable, transition from $P2_1/m$ to $C2/m$ symmetry [abstr.] *Amer. Mineral.* **55,** 305–306.

RABBITT, J. C. (1948) A new study of the anthophyllite series. *Amer. Mineral.* **33,** 263–323.

ROBINSON, P. (1966) Alumino-silicate polymorphs and Paleozoic erosion rates in central Massachusetts (abstr.). *Trans. Amer. Geophys. Union* **47,** 424.

———, AND H. W. JAFFE (1969a) Aluminous enclaves in gedrite-cordierite gneiss from southwestern New Hampshire. *Amer. Jour. Science* **267,** 389–421.

——— AND H. W. JAFFE (1969b) Chemographic exploration of amphibole assemblages from central Massachusetts and southwestern New Hampshire. *Mineral. Soc. Amer. Spec. Pap.* **2,** 251–274.

———, ———, C. KLEIN, AND M. ROSS (1969) Equilibrium coexistence of three amphiboles. *Contrib. Mineral. Petrol.* **22,** 248–258.

———, M. ROSS AND H. JAFFE (1970) The composition field of anthophyllite and the anthophyllite miscibility gap. (abstr.) *Amer. Mineral.* **55,** 307–309.

ROSS, M., J. J. PAPIKE, AND K. W. SHAW (1969) Exsolution textures in amphiboles as indicators of subsolidus thermal histories. *Mineral. Soc. Amer. Spec. Pap.* **2,** 275–299.

———, ———, AND P. W. WEIBLEN (1968) Exsolution in clinoamphiboles. *Science,* **159,** 1099–1104.

SMITH, J. V. (1954) A review of the Al-O and Si-O distances. *Acta Crystallogr.* **7,** 479–481.

——— AND S. W. BAILEY (1963) Second review of Al-O and Si-O tetrahedral distances. *Acta Crystallogr.* **16,** 801–811.

STOUT, J. H. (1969) An electron microprobe study of coexisting orthorhombic amphiboles. (abstr.) *Trans. Amer. Geophys. Union,* **50,** 359.

——— (1970) Three-amphibole assemblages and their bearing on the anthophyllite-gedrite miscibility gap. [abstr.] *Amer. Mineral.* **55,** 312–313.

THOMPSON, J. B. (1970) Geometrical possibilities for amphibole structures: Model biopyriboles (abstr.). *Amer. Mineral.* **55,** 292–293.

VIRGO, D. AND S. H. HAFNER (1969) Fe^{2+}, Mg Order-Disorder in heated orthopyroxenes. *Mineral. Soc. Amer. Spec. Pap.* **2,** 67–81.

WARREN, B. E. AND D. E. MODELL (1930) The structure of anthophyllite. *Z. Kristallogr.* **75,** 161–178.

WHITTAKER, E. J. W. (1969) The structure of the orthorhombic amphibole holmquistite. *Acta Crystallogr.* **B25,** 394–397.

Manuscript received, February 19, 1970; accepted for publication, July 22, 1970.